Retrosplenial Cortical Connectivity with Frontal Basal Ganglia Networks

Megan E. Monko and Sarah R. Heilbronner

Abstract

■ Previous studies of the retrosplenial cortex (RSC) have focused on its role in navigation and memory, consistent with its well-established medial temporal connections, but recent evidence also suggests a role for this region in reward and decision making. Because function is determined largely by anatomical connections, and to better understand the anatomy of RSC, we used tract-tracing methods to examine the anatomical connectivity between the rat RSC and frontostriatal networks (canonical reward and decision-making circuits). We find that, among frontal cortical regions, RSC bidirectionally connects most strongly with the anterior cingulate cortex, but also with an area of the central–medial orbito-frontal cortex. RSC projects to the dorsomedial striatum, and its terminal fields are virtually encompassed by the frontal-striatal projection zone, suggestive of functional convergence through the basal ganglia. This overlap is driven by anterior cingulate cortex, prelimbic cortex, and orbito-frontal cortex, all of which contribute to goal-directed decision making, suggesting that the RSC is involved in similar processes. ■

INTRODUCTION

The retrosplenial cortex (RSC) in rodents occupies a large territory in the posterior medial part of the cerebral cortex. Its strong connections with medial temporal lobe areas are well-established (Sugar, Witter, van Strien, & Cappaert, 2011; van Groen & Wyss, 1990, 1992, 2003). The prominence of these connections has motivated theorizing on RSC function, which has, not surprisingly, focused on spatial navigation and memory (Kaboodvand, Bäckman, Nyberg, & Salami, 2018; Auger & Maguire, 2013; Auger, Mullally, & Maguire, 2012; Keene & Bucci, 2008, 2009; Vann, Aggleton, & Maguire, 2009; Harker & Whishaw, 2004; Maviel, Durkin, Menzaghi, & Bontempi, 2004; Parron & Save, 2004; Cho & Sharp, 2001; Maguire, 2001; Cooper & Mizumori, 1999; Valenstein et al., 1987). For example, lesions in the RSC lead to deficits in performance on a water maze test (Sutherland, Wishaw, & Kolb, 1988) and to impairments in allocentric spatial memory (Pothuizen, Aggleton, & Vann, 2008; Vann & Aggleton, 2002, 2004).

However, RSC likely has a broader and more integrative function than is currently appreciated. In particular, there is compelling evidence that RSC may play a crucial role in reward-guided decision making (Hattori, Danskin, Babic, Mlynaryk, & Komiyama, 2019; Powell et al., 2017; Vedder, Miller, Harrison, & Smith, 2017; Nelson, Hindley, Haddon, Vann, & Aggleton, 2014; Tabuchi et al., 2005). For example, neural population activity in the RSC encodes a persistent value, with flexible reward history encoding (Hattori et al., 2019). In addition, the RSC plays a central albeit poorly delineated role in the default mode network (DMN), a network of functionally connected brain regions associated with high activity at rest, self-projection, episodic memory, and reward monitoring (Raichle et al., 2001; Shulman et al., 1997), which has been found in humans (Raichle et al., 2001), nonhuman primates (Mantini et al., 2011), and rodents (Lu et al., 2012; Upadhyay et al., 2011). Understanding the role of RSC is particularly important because it is likely to become a major research focus in the coming years: It reaches the dorsal surface of the brain and, therefore, is readily optically accessible to studies of neural activity using calcium imaging. Future work aimed at fully understanding the functions of RSC must take into account its roles in reward, decision making, and DMN processes. However, our ability to do so is limited by a lack of integrative knowledge of the anatomical connections of the RSC.

Most studies of reward-guided decision making implicate frontal cortico-striatal circuits (Fitoussi et al., 2018; Gremel et al., 2016; Sleezer, Castagno, & Hayden, 2016; Burton, Nakamura, & Roesch, 2015; Rothwell et al., 2015; Haber & Behrens, 2014; Yin, Knowlton, & Balleine, 2006; Balleine, Delgado, & Hikosaka, 2007; O'Doherty et al., 2004). The functions of these regions and projections are very well-studied using diverse tools, including lesions, optogenetics, electrophysiology, and pharmacology. Distinct striatal zones and their unique afferents have been implicated in different components of reward-guided decision making. Broadly speaking, there is consensus that the ventral striatum, dorsomedial striatum, and dorsolateral striatum, along with their frontal cortical afferents, have different roles in reward-guided decision making (Li et al., 2016; O'Hare et al., 2016; Kimchi & Laubach, 2009; Yin, Ostlund, Knowlton, & Balleine, 2005; Voorn, Vanderschuren, Groenewegen, Robbins, &

University of Minnesota, Twin Cities

Journal of Cognitive Neuroscience 33:6, pp. 1096–1105
https://doi.org/10.1162/jocn_a_01699

Pennartz, 2004; Yin & Knowlton, 2004; Hassani, Cromwell, & Schultz, 2001). One major hypothesis is that the dorsolateral striatum is involved with habits, the dorsomedial striatum is involved in goal-directed decision making, and the ventral striatum is involved in establishing stimulus-value associations.

One way to understand the function of the RSC in reward-guided decision making is to analyze its anatomical connections with this canonical, frontal cortico-striatal decision-making circuitry. Furthermore, the major subregions of the DMN are the RSC and portions of the frontal cortex, meaning the same cortical circuitry gives us insight into both reward-guided decision making and DMN function. Previous studies have demonstrated that there are significant projections between the RSC and the frontal cortex and striatum in rats (Shibata & Naito, 2008; Shibata, Kondo, & Naito, 2004; van Groen & Wyss, 1990, 1992, 2003). However, the projections to the striatum in particular have not been analyzed in detail, especially in light of our current understanding of how different zones of the striatum contribute to reward-guided decision making. Thus, in this paper, we used anatomical tract-tracing methods in rats to analyze the connections of the RSC with the striatum and frontal cortex.

METHODS

Overview

Connectivity of the RSC with the striatum and frontal cortical subregions was analyzed using anatomical tract-tracing in rats. Following surgery and perfusion, immunohistochemistry was performed and brain slices were mounted on slides. Labeling in the striatum (anterograde) and frontal cortex (anterograde and retrograde) were charted using light microscopy. Cases were registered to a standard brain for comparison and visualization.

Surgery and Tissue Preparation

All procedures were approved by the Institutional Animal Care and Use Committee at the University of Minnesota. Six adult male and five adult female Sprague Dawley rats (weight = 230–500 g, Charles River) were used for these studies.

At the start of surgery, animals were anesthetized using a combination of ketamine (40–90 mg/kg, intraperitoneal [IP]) and xylazine (5–10 mg/kg, IP). In addition, a nonsteroidal anti-inflammatory drug (Carprofen, 5 mg/kg, IP or subcutaneous [SQ]) and an antibiotic (Baytril, 2.5 mg/kg, SQ) were administered. Saline injections were given periodically to maintain hydration. Animals were placed in a stereotaxic frame on top of a heat source. Temperature and foot withdrawal reflex were monitored throughout to ensure stable anesthesia. Lidocaine was administered at the incision site. The skull was exposed, and then burr holes were made to expose the surface of the brain. The bidirectional tract-tracer fluororuby (FR, 40–50 nl, 10% in 0.1-M phosphate buffer, pH 7.4, Invitrogen) was injected over 10 min using a 0.5-μL Hamilton syringe. After each injection, the syringe remained in situ for 10–20 min. The syringe was removed, and the incision was closed with sutures. Atipamezole (0.1–1.0 mg/kg, IP) was used to reverse the ketamine/xylazine combination. Postoperatively, Carprofen (5 mg/kg, SQ) was delivered every 24 hr for 72 hr total. Targets were chosen using Paxinos and Watson (2014).

Animals were euthanized 10–14 days following injection with an IP injection of a lethal dose of commercial euthanasia solution (Euthasol, 0.22 mL/kg), and transcardially perfused with saline followed by 4% paraformaldehyde. Brains were extracted, postfixed overnight, and cryoprotected in increasing gradients of sucrose (10%, 20%, and 30%). Serial sections of 50 μm were cut on a freezing microtome into cryoprotectant solution. Serial sections of 50 μm were cut on a freezing microtome. One in six sections was processed free-floating for immunocytochemistry to visualize the tracer. Tissue was incubated in primary anti-FR (1:6000; Invitrogen) in 10% normal goat serum and 0.3% Triton X-100 (Sigma-Aldrich) in PO4 for 4 nights at 4°C. After rinsing, the tissue was incubated in biotinylated secondary antibody followed by incubation with the avidin-biotin complex solution (Vectastain ABC kit, Vector Laboratories). Immunoreactivity was then visualized using standard 3,3′-Diaminobenzidine (DAB) procedures. Staining was intensified by incubating the tissue for 5–15 sec in a solution of 0.05% tetrahydrochloride, 0.025% cobalt chloride, 0.02% nickel ammonium sulfate, and 0.01% H_2O_2. Sections were mounted by hand onto gel-coated slides, dehydrated, defatted in xylene, and coverslipped with Permount.

Microscopy and Analysis

Microscopy was performed using a Zeiss AxioImager M2 microscope. Three representative cases were chosen for in-depth analysis and 3-D rendering on the basis of their outstanding transport and lack of contamination. Using darkfield light microscopy, brain sections and structures, the injection site, and cortical and striatal terminal fields were outlined under a 2.0Å~, 4.0Å~, or 10× objective with Neurolucida software (MBF Bioscience). Terminal fields were considered dense when they could be visualized at a low objective (2.0×; criterion as previously utilized in Heilbronner, Meyer, Choi, & Haber, 2018; Heilbronner & Haber, 2014; Haynes & Haber, 2013; Mailly, Aliane, Groenewegen, Haber, & Deniau, 2013; Haber, Kim, Mailly, & Calzavara, 2006). We distinguished between likely terminal fields (thin, labeled fibers containing boutons) and passing fibers (thick fibers without clear boutons). In addition, using brightfield light microscopy, retrogradely labeled cells (all within the target region) were counted using StereoInvestigator software (MBF Bioscience) under a 20× objective. This stereology software was utilized to ensure that every part of a region received equal attention and to avoid biases associated with dark staining and cell

clusters. We analyzed one out of every six sections, and density was defined by total number of cells normalized by brain region size, with size defined by the sum of the areas of the brain regions across the one in six sections, rather than by volume.

For each case, stacks of coronal sections were created from chartings and scanned slides. These stacks were imported into IMOD software (Boulder Laboratory for 3-D Electron Microscopy; Kremer, Mastronarde, & McIntosh, 1996) and combined, and thus, a 3-D reconstruction that contained the injection sites, terminal fields, and labeled cells was created for each case separately. To merge multiple cases together, individual cases were registered in IMOD to standard rat MRI images that had been converted to IMOD files (Wisner, Odintsov, Brozoski, & Brozoski, 2016). Registrations were manually checked and adjusted according to cortical and striatal landmarks.

We wanted to compare the RSC-striatal projection zone to previously established frontal-striatal projection zones. Projection zones for areas CG (anterior cingulate cortex), PL (prelimbic cortex), MO (medial orbito-frontal cortex), VOLO (ventral and lateral orbito-frontal cortex), and IL (infralimbic cortex) were drawn from Heilbronner, Rodriguez-Romaguera, Quirk, Groenewegen, and Haber (2016). In that paper, we combined prior maps of cortico-striatal projection fields, with a focus on the projections at anterior–posterior distance from bregma (AP) +1.1, where the frontal terminal fields appeared to be maximally segregated. The database consisted of four cases from IL, 10 from PL, five from CG, three from MO, and nine from VOLO. To this database, we added projections from area M2 (three cases) as depicted in Reep and Corwin (1999). Overlaps in terminal field areas at three coronal A-P positions were calculated by converting the pixels of the models in IMOD to a polygon and finding the area of the intersect using custom MATLAB (The MathWorks) code.

RESULTS

The cases included in these analyses had the bidirectional tracer FR injected into the RSC. Resulting injection sites were confined to the RSC and, together, covered most of its rostral-caudal length (collectively the cores of the injection sites ranged from −4.8 to −8.8 AP). We first analyzed the projections from the RSC to the striatum. Like most cortical areas, the RSC projects to both ipsilateral and contralateral striatum with predominance of the former (McGeorge

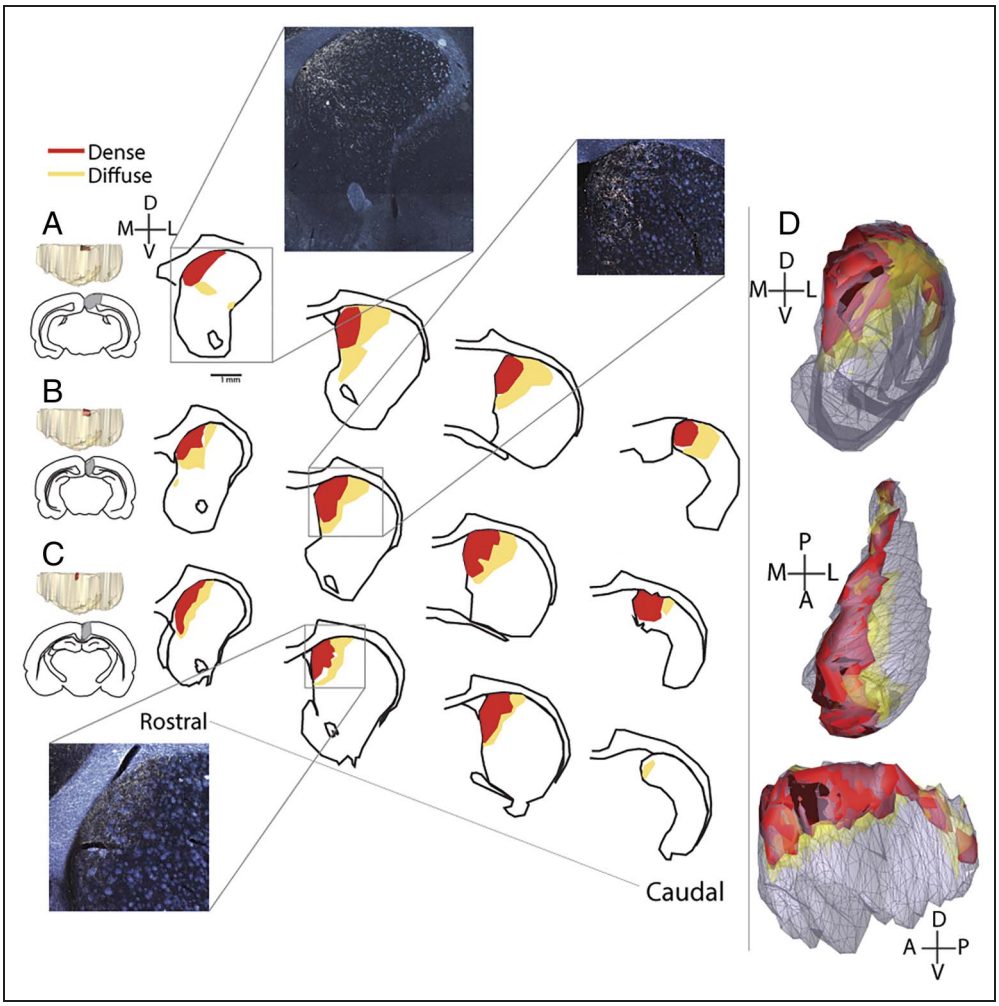

Figure 1. RSC-striatal terminal fields. Images at far left show 3-D models and outlines for the three injection sites (A–C). The coordinates of the spread of the injection sites in the anterior/posterior direction are A. −4.8 to −8.6 AP, B. −4.8 to −8.8 AP, and C. −5.0 to −6.0 AP. Drawings show coronal striatal sections with terminal fields from rostral to caudal striatum. Photomicrographs show coronal darkfield images of ipsilateral striatal terminal fields. White arrows point to dense terminal fields. (D) Collective model of the striatal projection zone of the RSC from coronal (top), horizontal (middle), and sagittal (bottom) views, all cases combined. Scale bar = 1 mm.

& Faull, 1989). Therefore, we analyzed ipsilateral striatal projections, but there were similarly situated, less dense, contralateral terminal fields as well. Cases were extremely similar in their striatal projections and, thus, are described here together. Fibers could be visualized exiting the injection site and traveling ventrally and rostrally toward the dorsal striatum through the cingulum bundle and the white matter directly adjacent to it. These fibers formed longitudinal bands of terminal fields that extended for nearly the entire rostral-caudal distance of the ipsilateral caudoputamen. At the most caudal levels of the caudoputamen, terminal fields were present only dorsally. Rostrally, where the caudoputamen widens in the medial-lateral dimension, terminal fields were restricted to the dorsomedial component. They frequently reached the dorsomedial boundary between the caudoputamen and the lateral ventricle (Figure 1). In all cases, both dense and diffuse projections could be observed. The dense projections were the most consistently dorsomedial, whereas the lighter projections extended further ventrally and laterally. However, even diffuse projections did not extend into the nucleus accumbens.

Next, we examined connections between RSC and different regions within the frontal cortex (Figure 2). Although there were some quantitative differences between the cases (Figure 2D), qualitatively, we observed consistent bidirectional connections primarily with the dorsal anterior cingulate areas (CG1, CG2, and A33) and a specific location within the central-medial orbito-frontal cortex that sits at the border between ventral orbital and MO. Much weaker, but present, connections were observed with IL, PL, M2, and M1. Virtually no connectivity was observed with lateral orbito-frontal cortex and frontal insular regions. Thus, although there is a consistent patch of connectivity in the central-medial orbito-frontal cortex, the medial frontal

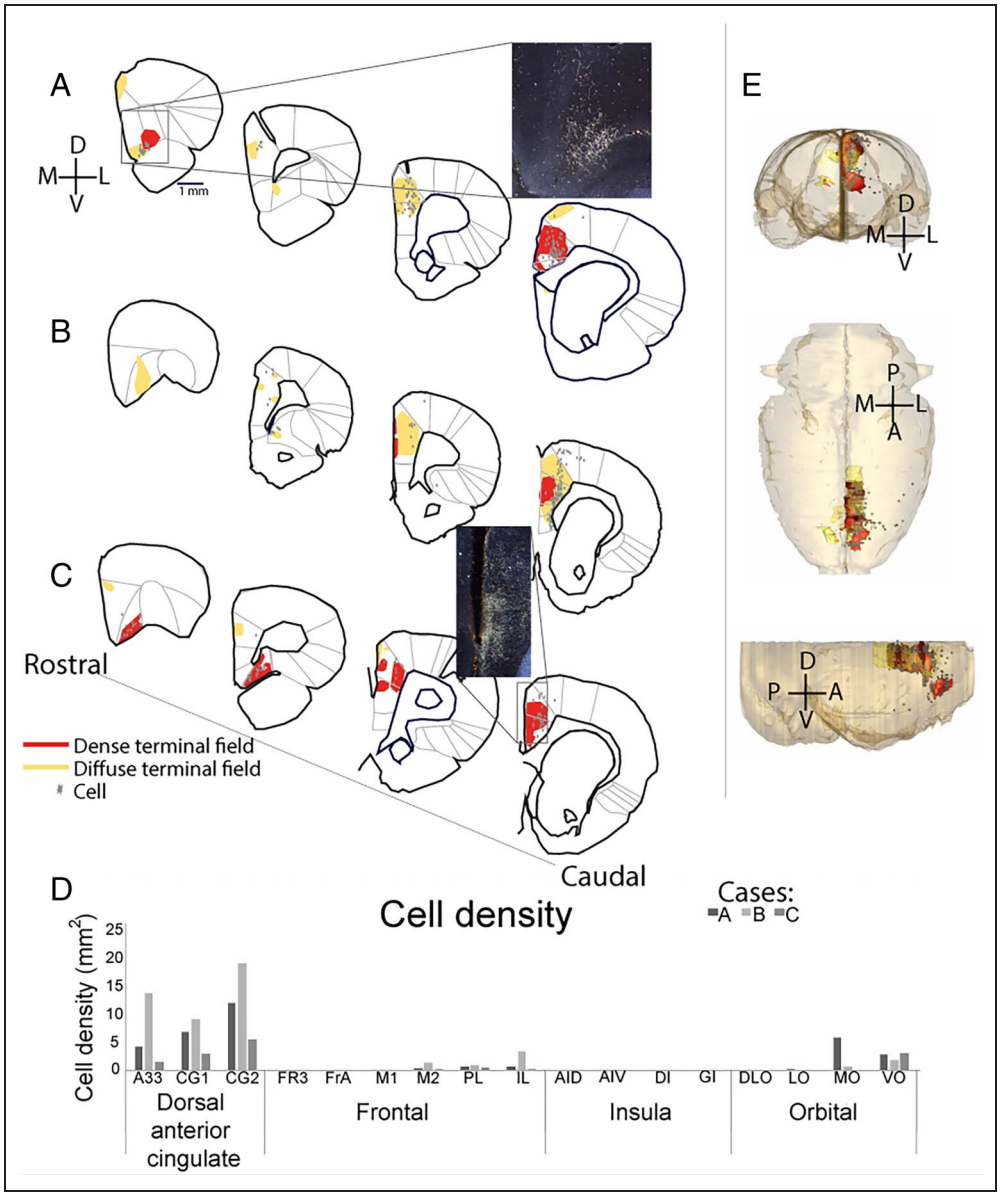

Figure 2. RSC-frontal projections. Terminal fields and labeled cells following injections into the RSC, (A–C) Drawings of frontal terminal fields (red = dense terminal fields, yellow = diffuse terminal fields; gray dots = cells; all shown for each injection site). (Each case is a different injection site, matched to Figure 1.) (D) Cell density from each case in frontal regions. Results are shown for each case (A–C, as above). (E) Collective model of the frontal projections of the RSC from coronal (top), horizontal (middle), and sagittal (bottom) views, all cases combined. Scale bar = 1 mm.

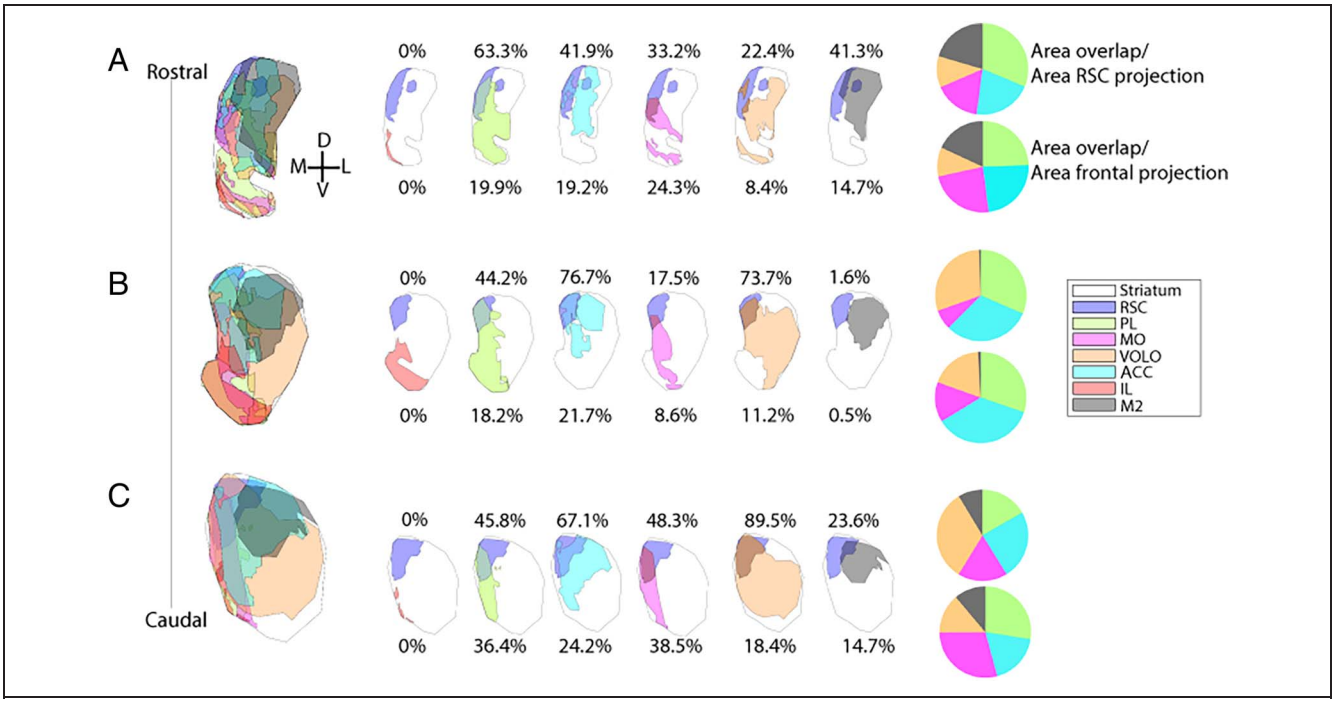

Figure 3. Cortico-striatal overlap. Analyses of overlap of the RSC projection zone in the striatum with select frontal area projection zones. Drawings depict the RSC projection zone (purple) at AP +2.3 (A), AP +1.1 (B), and AP −0.1 (C) compared to IL (red), PL (yellow-green), CG (light blue), MO (purple), VOLO (orange), and M2 (black) projection zones. Numbers and pie charts show the area of the RSC-striatal projection zone encapsulated within the frontal area's projection zone, divided by the area of the RSC projection (top) or the area of the frontal projection (bottom). AP = anterior–posterior distance from bregma; IL = infralimbic cortex; PL = prelimbic cortex; CG = anterior cingulate cortex; MO = medial orbital cortex; VOLO = ventral and lateral orbital cortex.

cortex has, overall, much stronger connections with the RSC than the orbito-frontal cortex does. In addition, in both the medial and orbito-frontal cortices, RSC connectivity is with the central portions, rather than the ventral/dorsal or medial/lateral edges.

We then analyzed the overlap between the striatal terminal fields from the RSC and the striatal projection zones of various frontal regions, as previously defined (Heilbronner et al., 2016; Reep & Corwin, 1999; Figure 3). At all A-P levels examined, the RSC does not occupy striatal territory isolated from frontal projections. Instead, large portions of the RSC projection zone overlap with terminal fields from frontal cortical regions (at A-P +2.3, > 90%; at A-P +1.1 > 95%; at A-P −0.1, > 98%). At A-P +1.1, the database of frontal terminal fields is greatest, and the projection zones from these regions are maximally segregated, so we will consider this topography in detail here (although note other levels diagrammed in Figure 3). The greatest percentage of overlap is with central–medial prefrontal regions (prelimbic and anterior cingulate cortices) and central and lateral orbito-frontal regions. Smaller zones of overlap are observed between the RSC projection zones and those from M2 and MO. At this level and all levels, there is no overlap between the RSC projection zone and the infralimbic projection zone. Finally, although the RSC-striatal projection is not isolated from frontal-striatal projections, no frontal-striatal projection zone is as uniquely confined to the dorsomedial caudoputamen as the RSC terminal fields are.

DISCUSSION

Here, we examined in detail the projections of the RSC to frontal cortico-basal ganglia circuits. We found that the RSC projects exclusively to the dorsomedial striatum, which also receives dense projections from dorsal anterior cingulate, ventral and lateral orbital areas, and prelimbic cortex. The RSC has bidirectional connections with dorsal anterior cingulate regions, central-medial orbito-frontal cortex, and, to a lesser extent, PL and IL. These results are in full agreement with prior anatomical work in both rats and mice (Hintiryan et al., 2016; Hunnicutt et al., 2016; Shibata & Naito, 2008; Shibata et al., 2004; Cheatwood, Reep, & Corwin, 2003; Reep, Cheatwood, & Corwin, 2003; van Groen & Wyss, 1992, 2003); here, our goal was to synthesize frontal and striatal projections from a functional perspective.

While RSC has historically been known for its role in navigation and memory functions likely shared with the medial temporal lobe, it also seems to play an important role in reward-guided decision making, a process that is most commonly associated with frontal cortico-basal ganglia regions and circuits. The dorsomedial striatum and its frontal cortical afferents are known to be involved with goal-directed decision making rather than stimulus value or procedural learning. For example, inhibition of orbito-frontal-dorsomedial striatal neurons caused mice to be unable to shift to goal-directed action control (Gremel et al.,

2016). The placement of RSC within this circuitry calls for similar manipulation studies focused on testing the role of RSC-striatal neurons in goal-directed behavior.

The RSC has mainly been studied in the context of spatial navigation and memory due in part to its strong anatomical connectivity with medial temporal lobe structures (Mitchell, Czajkowski, Zhang, Jeffery, & Nelson, 2018; Vann et al., 2009). The cortico-basal ganglia loops of the medial temporal lobe are both distinct and overlapping with those of the RSC. The hippocampus, for example, projects mainly to the medial nucleus accumbens, positioning it quite differently than the RSC projection (Groenewegen, Vermeulen-Van der Zee, te Kortschot, & Witter, 1987). However, very rostrally in the caudoputamen, the hippocampus projects just laterally to the lateral ventricle, similar to the rostral RSC-striatal projection zone. Similarly, entorhinal and perirhinal cortices primarily project to the nucleus accumbens, but also dorsal and medial borders of the caudoputamen, overlapping with the RSC projection zone (McIntyre, Kelly, & Staines, 1996; McGeorge & Faull, 1989). Taken together, the bulk of the medial temporal lobe structures project mainly to the nucleus accumbens, yet these structures do also project to the dorsomedial caudoputamen in such a way as to provide some overlap with the RSC projection zone there, although this overlap is not consistent across rostral versus caudal caudoputamen. Similarly, with the exception of perirhinal cortex, medial temporal lobe frontal projections are more strongly connected with ventral prefrontal cortex, rather than dorsal (Insausti, Herrero, & Witter, 1997; Verwer, Meijer, Van Uum, & Witter, 1997; McIntyre et al., 1996; Jay, Glowinski, & Thierry, 1989).

RSC-frontal projections mostly parallel the striatal projection zone overlap. Cortico-basal ganglia loops have been described as both parallel (Miyachi, 2009; Alexander, DeLong, & Strick, 1986) and integrative (Groenewegen, Voorn, & Scheel-Krüger, 2016; Draganski et al., 2008; Haber et al., 2006). Furthermore, tract-tracing experiments have found that connected cortical areas overlap in their striatal terminal fields (Selemon & Goldman-Rakic, 1985), creating a network with some unifying function (Selemon & Goldman-Rakic, 1988). This concept has been extended to human resting-state functional connectivity, in which distributed, correlated activity defines such functional networks as the DMN, the dorsal attention network, and the frontoparietal network (Choi, Yeo, & Buckner, 2012; Yeo et al., 2011). Here, we find that, in rats, projections between the RSC and the frontal lobe roughly, but do not precisely, match the overlap in terminal fields in the striatum. CG, for example, projects to the dorsomedial and dorsocentral striatum, overlapping considerably with the RSC striatal-projection zone, and also has strong connections with the RSC. The IL, by contrast, does not overlap with the RSC-striatal projection zone and has only very weak connections with the RSC. However, the PL has only weak connections with the RSC but projects strongly to the dorsomedial striatum. One possibility is that this connection serves an integrative function for decision-making processes at the level of the basal ganglia. This integrative function might relate to the RSC's function in navigation, providing information about location to the areas that are involved in decision making.

The human RSC is part of the larger structure of the posteromedial cortex, which is the main hub of the DMN. This network, which is more active during resting states than cognitive tasks (Greicius, Krasnow, Reiss, & Menon, 2003), also includes frontal and temporal regions. Mirroring the RSC-striatal anatomical connections in rats, the DMN is functionally connected with the medial caudate in humans (Choi et al., 2012). The DMN in rodents, which includes the RSC (Lu et al., 2012; Upadhyay et al., 2011), the central-medial orbito-frontal cortex, and the dorsomedial frontal cortex, seems to closely match the anatomical connectivity pattern shown here. A new theory of the role of the DMN posits that, in monkeys, much of the DMN participates in cognitive shifting (Arsenault, Caspari, Vandenberghe, & Vanduffel, 2018). Therefore, one possibility is that the RSC is involved in attentional shifting in rodents as a function of its striatal territory. As a hub of the DMN, RSC in humans is known to be impaired in various psychiatric and neurological disorders (Doucet et al., 2020; He et al., 2018; Satyshur, Layden, Gowins, Buchanan, & Gollan, 2018; Martino et al., 2016; Wu et al., 2016; Baker et al., 2014; Cowdrey, Filippini, Park, Smith, & McCabe, 2014; Hafkemeijer, van der Grond, & Rombouts, 2012; Anderson et al., 2011; Bluhm et al., 2009). Understanding the biology of the DMN will require a detailed, translational explication of the functional roles of the RSC, not just in navigation and memory, but also in decision making.

Acknowledgments

We thank Tanya Casta, Adriana Cushnie, Mark Grier, and Anish Sethi for assistance with data collection. This work was supported by the National Institute of Mental Health (R01118257), the MnDrive Brain Conditions Initiative, and the Brain & Behavior Research Foundation.

Reprint requests should be sent to Sarah Heilbronner, Department of Neuroscience, University of Minnesota, 2-164 Jackson Hall, 321 Church St SE, Minneapolis, MN 5545, or via e-mail: heilb028@umn.edu.

Author Contributions

Megan E. Monko: Conceptualization; Data curation; Formal analysis; Investigation; Project administration; Visualization; Writing—Original draft; Writing—Review & editing. Sarah R. Heilbronner: Conceptualization; Formal analysis; Funding acquisition; Investigation; Methodology; Project administration; Supervision; Visualization; Writing—Original draft; Writing—Review & editing.

Funding Information

National Institute of Mental Health (http://dx.doi.org/10.13039/100000025), grant number: R01118257. Brain and

Behavior Research Foundation (http://dx.doi.org/10.13039/100000874), grant number: NARSAD Young Investigator Award. MnDrive Brain Conditions Initiative.

Diversity in Citation Practices

A retrospective analysis of the citations in every article published in this journal from 2010 to 2020 has revealed a persistent pattern of gender imbalance: Although the proportions of authorship teams (categorized by estimated gender identification of first author/last author) publishing in the *Journal of Cognitive Neuroscience (JoCN)* during this period were M(an)/M = .408, W(oman)/M = .335, M/W = .108, and W/W = .149, the comparable proportions for the articles that these authorship teams cited were M/M = .579, W/M = .243, M/W = .102, and W/W = .076 (Fulvio et al., *JoCN*, 33:1, pp. 3–7). Consequently, *JoCN* encourages all authors to consider gender balance explicitly when selecting which articles to cite and gives them the opportunity to report their article's gender citation balance.

REFERENCES

Alexander, G. E., DeLong, M. R., & Strick, P. L. (1986). Parallel organization of functionally segregated circuits linking basal ganglia and cortex. *Annual Review of Neuroscience*, *9*, 357–381. **DOI:** https://doi.org/10.1146/annurev.ne.09.030186.002041, **PMID:** 3085570

Anderson, J. S., Druzgal, T. J., Lopez-Larson, M., Jeong, E.-K., Desai, K., & Yurgelun-Todd, D. (2011). Network anticorrelations, global regression, and phase-shifted soft tissue correction. *Human Brain Mapping*, *32*, 919–934. **DOI:** https://doi.org/10.1002/hbm.21079, **PMID:** 20533557, **PMCID:** PMC3220164

Arsenault, J. T., Caspari, N., Vandenberghe, R., & Vanduffel, W. (2018). Attention shifts recruit the monkey default mode network. *Journal of Neuroscience*, *38*, 1202–1217. **DOI:** https://doi.org/10.1523/JNEUROSCI.1111-17.2017, **PMID:** 29263238, **PMCID:** PMC6596261

Auger, S. D., & Maguire, E. A. (2013). Assessing the mechanism of response in the retrosplenial cortex of good and poor navigators. *Cortex*, *49*, 2904–2913. **DOI:** https://doi.org/10.1016/j.cortex.2013.08.002, **PMID:** 24012136, **PMCID:** PMC3878422

Auger, S. D., Mullally, S. L., & Maguire, E. A. (2012). Retrosplenial cortex codes for permanent landmarks. *PLoS One*, *7*, e43620. **DOI:** https://doi.org/10.1371/journal.pone.0043620, **PMID:** 22912894, **PMCID:** PMC3422332

Baker, J. T., Holmes, A. J., Masters, G. A., Yeo, B. T. T., Krienen, F., Buckner, R. L., et al. (2014). Disruption of cortical association networks in schizophrenia and psychotic bipolar disorder. *JAMA Psychiatry*, *71*, 109–118. **DOI:** https://doi.org/10.1001/jamapsychiatry.2013.3469, **PMID:** 24306091, **PMCID:** PMC4435541

Balleine, B. W., Delgado, M. R., & Hikosaka, O. (2007). The role of the dorsal striatum in reward and decision-making. *Journal of Neuroscience*, *27*, 8161–8165. **DOI:** https://doi.org/10.1523/JNEUROSCI.1554-07.2007, **PMID:** 17670959, **PMCID:** PMC6673072

Bluhm, R., Williamson, P., Lanius, R., Théberge, J., Densmore, M., Bartha, R., et al. (2009). Resting state default-mode network connectivity in early depression using a seed region-of-interest analysis: Decreased connectivity with caudate nucleus. *Psychiatry and Clinical Neurosciences*, *63*, 754–761. **DOI:** https://doi.org/10.1111/j.1440-1819.2009.02030.x, **PMID:** 20021629

Burton, A. C., Nakamura, K., & Roesch, M. R. (2015). From ventral-medial to dorsal-lateral striatum: Neural correlates of reward-guided decision-making. *Neurobiology of Learning and Memory*, *117*, 51–59. **DOI:** https://doi.org/10.1016/j.nlm.2014.05.003, **PMID:** 24858182, **PMCID:** PMC4240773

Cheatwood, J. L., Reep, R. L., & Corwin, J. V. (2003). The associative striatum: Cortical and thalamic projections to the dorsocentral striatum in rats. *Brain Research*, *968*, 1–14. **DOI:** https://doi.org/10.1016/S0006-8993(02)04212-9, **PMID:** 12644259

Cho, J., & Sharp, P. E. (2001). Head direction, place, and movement correlates for cells in the rat retrosplenial cortex. *Behavioral Neuroscience*, *115*, 3–25. **DOI:** https://doi.org/10.1037/0735-7044.115.1.3, **PMID:** 11256450

Choi, E. Y., Yeo, B. T. T., & Buckner, R. L. (2012). The organization of the human striatum estimated by intrinsic functional connectivity. *Journal of Neurophysiology*, *108*, 2242–2263. **DOI:** https://doi.org/10.1152/jn.00270.2012, **PMID:** 22832566, **PMCID:** PMC3545026

Cooper, B. G., & Mizumori, S. J. (1999). Retrosplenial cortex inactivation selectively impairs navigation in darkness. *NeuroReport*, *10*, 625–630. **DOI:** https://doi.org/10.1097/00001756-199902250-00033, **PMID:** 10208601

Cowdrey, F. A., Filippini, N., Park, R. J., Smith, S. M., & McCabe, C. (2014). Increased resting state functional connectivity in the default mode network in recovered anorexia nervosa. *Human Brain Mapping*, *35*, 483–491. **DOI:** https://doi.org/10.1002/hbm.22202, **PMID:** 23033154, **PMCID:** PMC6869597

Doucet, G. E., Janiri, D., Howard, R., O'Brien, M., Andrews-Hanna, J. R., & Frangou, S. (2020). Transdiagnostic and disease-specific abnormalities in the default-mode network hubs in psychiatric disorders: A meta-analysis of resting-state functional imaging studies. *European Psychiatry*, *63*, e57. **DOI:** https://doi.org/10.1192/j.eurpsy.2020.57, **PMID:** 32466812, **PMCID:** PMC7355168

Draganski, B., Kherif, F., Klöppel, S., Cook, P. A., Alexander, D. C., Parker, G. J. M., et al. (2008). Evidence for segregated and integrative connectivity patterns in the human basal ganglia. *Journal of Neuroscience*, *28*, 7143–7152. **DOI:** https://doi.org/10.1523/JNEUROSCI.1486-08.2008, **PMID:** 18614684, **PMCID:** PMC6670486

Fitoussi, A., Renault, P., Le Moine, C., Coutureau, E., Cador, M., & Dellu-Hagedorn, F. (2018). Inter-individual differences in decision-making, flexible and goal-directed behaviors: Novel insights within the prefronto-striatal networks. *Brain Structure & Function*, *223*, 897–912. **DOI:** https://doi.org/10.1007/s00429-017-1530-z, **PMID:** 29026986

Greicius, M. D., Krasnow, B., Reiss, A. L., & Menon, V. (2003). Functional connectivity in the resting brain: A network analysis of the default mode hypothesis. *Proceedings of the National Academy of Sciences, U.S.A.*, *100*, 253–258. **DOI:** https://doi.org/10.1073/pnas.0135058100, **PMID:** 12506194, **PMCID:** PMC140943

Gremel, C. M., Chancey, J. H., Atwood, B. K., Luo, G., Neve, R., Ramakrishnan, C., et al. (2016). Endocannabinoid modulation of orbitostriatal circuits gates habit formation. *Neuron*, *90*, 1312–1324. **DOI:** https://doi.org/10.1016/j.neuron.2016.04.043, **PMID:** 27238866, **PMCID:** PMC4911264

Groenewegen, H. J., Vermeulen-Van der Zee, E., te Kortschot, A., & Witter, M. P. (1987). Organization of the projections from the subiculum to the ventral striatum in the rat. A study using anterograde transport of Phaseolus vulgaris leucoagglutinin. *Neuroscience*, *23*, 103–120. **DOI:** https://doi.org/10.1016/0306-4522(87)90275-2, **PMID:** 3683859

Groenewegen, H. J., Voorn, P., & Scheel-Krüger, J. (2016). Limbic-basal ganglia circuits parallel and integrative aspects. In J.-J. Soghomonian (Ed.), *The basal ganglia: Innovations in cognitive neuroscience* (pp. 11–45). Cham: Springer. **DOI:** https://doi.org/10.1007/978-3-319-42743-0_2

Haber, S. N., & Behrens, T. E. J. (2014). The neural network underlying incentive-based learning: Implications for interpreting circuit disruptions in psychiatric disorders. *Neuron*, *83*, 1019–1039. **DOI:** https://doi.org/10.1016/j.neuron.2014.08.031, **PMID:** 25189208, **PMCID:** PMC4255982

Haber, S. N., Kim, K.-S., Mailly, P., & Calzavara, R. (2006). Reward-related cortical inputs define a large striatal region in primates that interface with associative cortical connections, providing a substrate for incentive-based learning. *Journal of Neuroscience*, *26*, 8368–8376. **DOI:** https://doi.org/10.1523/JNEUROSCI.0271-06.2006, **PMID:** 16899732, **PMCID:** PMC6673798

Hafkemeijer, A., van der Grond, J., & Rombouts, S. A. R. B. (2012). Imaging the default mode network in aging and dementia. *Biochimica et Biophysica Acta*, *1822*, 431–441. **DOI:** https://doi.org/10.1016/j.bbadis.2011.07.008, **PMID:** 21807094

Harker, K. T., & Whishaw, I. Q. (2004). Impaired place navigation in place and matching-to-place swimming pool tasks follows both retrosplenial cortex lesions and cingulum bundle lesions in rats. *Hippocampus*, *14*, 224–231. **DOI:** https://doi.org/10.1002/hipo.10159, **PMID:** 15098727

Hassani, O. K., Cromwell, H. C., & Schultz, W. (2001). Influence of expectation of different rewards on behavior-related neuronal activity in the striatum. *Journal of Neurophysiology*, *85*, 2477–2489. **DOI:** https://doi.org/10.1152/jn.2001.85.6.2477, **PMID:** 11387394

Hattori, R., Danskin, B., Babic, Z., Mlynaryk, N., & Komiyama, T. (2019). Area-specificity and plasticity of history-dependent value coding during learning. *Cell*, *177*, 1858–1872. **DOI:** https://doi.org/10.1016/j.cell.2019.04.027, **PMID:** 31080067, **PMCID:** PMC6663310

Haynes, W. I. A., & Haber, S. N. (2013). The organization of prefrontal-subthalamic inputs in primates provides an anatomical substrate for both functional specificity and integration: Implications for basal ganglia models and deep brain stimulation. *Journal of Neuroscience*, *33*, 4804–4814. **DOI:** https://doi.org/10.1523/JNEUROSCI.4674-12.2013, **PMID:** 23486951, **PMCID:** PMC3755746

He, C., Chen, Y., Jian, T., Chen, H., Guo, X., Wang, J., et al. (2018). Dynamic functional connectivity analysis reveals decreased variability of the default-mode network in developing autistic brain. *Autism Research*, *11*, 1479–1493. **DOI:** https://doi.org/10.1002/aur.2020, **PMID:** 30270547

Heilbronner, S. R., & Haber, S. N. (2014). Frontal cortical and subcortical projections provide a basis for segmenting the cingulum bundle: Implications for neuroimaging and psychiatric disorders. *Journal of Neuroscience*, *34*, 10041–10054. **DOI:** https://doi.org/10.1523/JNEUROSCI.5459-13.2014, **PMID:** 25057206, **PMCID:** PMC4107396

Heilbronner, S. R., Meyer, M. A. A., Choi, E. Y., & Haber, S. N. (2018). How do cortico-striatal projections impact on downstream pallidal circuitry? *Brain Structure & Function*, *223*, 2809–2821. **DOI:** https://doi.org/10.1007/s00429-018-1662-9, **PMID:** 29654360

Heilbronner, S. R., Rodriguez-Romaguera, J., Quirk, G. J., Groenewegen, H. J., & Haber, S. N. (2016). Circuit-based corticostriatal homologies between rat and primate. *Biological Psychiatry*, *80*, 509–521. **DOI:** https://doi.org/10.1016/j.biopsych.2016.05.012, **PMID:** 27450032, **PMCID:** PMC5438202

Hintiryan, H., Foster, N. N., Bowman, I., Bay, M., Song, M. Y., Gou, L., et al. (2016). The mouse cortico-striatal projectome. *Nature Neuroscience*, *19*, 1100–1114. **DOI:** https://doi.org/10.1038/nn.4332, **PMID:** 27322419, **PMCID:** PMC5564682

Hunnicutt, B. J., Jongbloets, B. C., Birdsong, W. T., Gertz, K. J., Zhong, H., & Mao, T. (2016). A comprehensive excitatory input map of the striatum reveals novel functional organization. *eLife*, *5*, e19103. **DOI:** https://doi.org/10.7554/eLife.19103, **PMID:** 27892854, **PMCID:** PMC5207773

Insausti, R., Herrero, M. T., & Witter, M. P. (1997). Entorhinal cortex of the rat: Cytoarchitectonic subdivisions and the origin and distribution of cortical efferents. *Hippocampus*, *7*, 146–183. **DOI:** https://doi.org/10.1002/(SICI)1098-1063(1997)7:2<146::AID-HIPO4>3.0.CO;2-L, **PMID:** 9136047

Jay, T. M., Glowinski, J., & Thierry, A. M. (1989). Selectivity of the hippocampal projection to the prelimbic area of the prefrontal cortex in the rat. *Brain Research*, *505*, 337–340. **DOI:** https://doi.org/10.1016/0006-8993(89)91464-9

Kaboodvand, N., Bäckman, L., Nyberg, L., & Salami, A. (2018). The retrosplenial cortex: A memory gateway between the cortical default mode network and the medial temporal lobe. *Human Brain Mapping*, *39*, 2020–2034. **DOI:** https://doi.org/10.1002/hbm.23983, **PMID:** 29363256, **PMCID:** PMC6866613

Keene, C. S., & Bucci, D. J. (2008). Neurotoxic lesions of retrosplenial cortex disrupt signaled and unsignaled contextual fear conditioning. *Behavioral Neuroscience*, *122*, 1070–1077. **DOI:** https://doi.org/10.1037/a0012895, **PMID:** 18823164

Keene, C. S., & Bucci, D. J. (2009). Damage to the retrosplenial cortex produces specific impairments in spatial working memory. *Neurobiology of Learning and Memory*, *91*, 408–414. **DOI:** https://doi.org/10.1016/j.nlm.2008.10.009, **PMID:** 19026755

Kimchi, E. Y., & Laubach, M. (2009). Dynamic encoding of action selection by the medial striatum. *Journal of Neuroscience*, *29*, 3148–3159. **DOI:** https://doi.org/10.1523/JNEUROSCI.5206-08.2009, **PMID:** 19279252, **PMCID:** PMC3415331

Kremer, J. R., Mastronarde, D. N., & McIntosh, J. R. (1996). Computer visualization of three-dimensional image data using IMOD. *Journal of Structural Biology*, *116*, 71–76. **DOI:** https://doi.org/10.1006/jsbi.1996.0013, **PMID:** 8742726

Li, Y., He, Y., Chen, M., Pu, Z., Chen, L., Li, P., et al. (2016). Optogenetic activation of adenosine A2A receptor signaling in the dorsomedial striatopallidal neurons suppresses goal-directed behavior. *Neuropsychopharmacology*, *41*, 1003–1013. **DOI:** https://doi.org/10.1038/npp.2015.227, **PMID:** 26216520, **PMCID:** PMC4748425

Lu, H., Zou, Q., Gu, H., Raichle, M. E., Stein, E. A., & Yang, Y. (2012). Rat brains also have a default mode network. *Proceedings of the National Academy of Sciences, U.S.A.*, *109*, 3979–3984. **DOI:** https://doi.org/10.1073/pnas.1200506109, **PMID:** 22355129, **PMCID:** PMC3309754

Maguire, E. A. (2001). The retrosplenial contribution to human navigation: A review of lesion and neuroimaging findings. *Scandinavian Journal of Psychology*, *42*, 225–238. **DOI:** https://doi.org/10.1111/1467-9450.00233, **PMID:** 11501737

Mailly, P., Aliane, V., Groenewegen, H. J., Haber, S. N., & Deniau, J.-M. (2013). The rat prefrontostriatal system analyzed in 3D: Evidence for multiple interacting functional units. *Journal of Neuroscience*, *33*, 5718–5727. **DOI:** https://doi.org/10.1523/JNEUROSCI.5248-12.2013, **PMID:** 23536085, **PMCID:** PMC6705071

Mantini, D., Gerits, A., Nelissen, K., Durand, J.-B., Joly, O., Simone, L., et al. (2011). Default mode of brain function in monkeys. *Journal of Neuroscience*, *31*, 12954–12962. **DOI:** https://doi.org/10.1523/JNEUROSCI.2318-11.2011, **PMID:** 21900574, **PMCID:** PMC3686636

Martino, M., Magioncalda, P., Huang, Z., Conio, B., Piaggio, N., Duncan, N. W., et al. (2016). Contrasting variability patterns in the default mode and sensorimotor networks balance in bipolar depression and mania. *Proceedings of National Academy of Sciences, U.S.A.*, *113*, 4824–4829. **DOI:** https://doi.org/10.1073/pnas.1517558113, **PMID:** 27071087, **PMCID:** PMC4855585

Maviel, T., Durkin, T. P., Menzaghi, F., & Bontempi, B. (2004). Sites of neocortical reorganization critical for remote spatial memory. *Science*, *305*, 96–99. **DOI:** https://doi.org/10.1126/science.1098180, **PMID:** 15232109

McGeorge, A. J., & Faull, R. L. (1989). The organization of the projection from the cerebral cortex to the striatum in the rat. *Neuroscience*, *29*, 503–537. **DOI:** https://doi.org/10.1016/0306-4522(89)90128-0, **PMID:** 2472578

McIntyre, D. C., Kelly, M. E., & Staines, W. A. (1996). Efferent projections of the anterior perirhinal cortex in the rat. *Journal of Comparative Neurology*, *369*, 302–318. **DOI:** https://doi.org/10.1002/(SICI)1096-9861(19960527)369:2<302::AID-CNE10>3.0.CO;2-J, **PMID:** 8727002

Mitchell, A. S., Czajkowski, R., Zhang, N., Jeffery, K., & Nelson, A. J. D. (2018). Retrosplenial cortex and its role in spatial cognition. *Brain and Neuroscience Advances*, *2*, 2398212818757098. **DOI:** https://doi.org/10.1177/2398212818757098, **PMID:** 30221204, **PMCID:** PMC6095108

Miyachi, S. (2009). Cortico-basal ganglia circuits—Parallel closed loops and convergent/divergent connections. *Brain and Nerve*, *61*, 351–359. **DOI:** https://doi.org/10.11477/mf.1416100459, **PMID:** 19378804

Nelson, A. J. D., Hindley, E. L., Haddon, J. E., Vann, S. D., & Aggleton, J. P. (2014). A novel role for the rat retrosplenial cortex in cognitive control. *Learning & Memory*, *21*, 90–97. **DOI:** https://doi.org/10.1101/lm.032136.113, **PMID:** 24434870, **PMCID:** PMC3895227

O'Doherty, J., Dayan, P., Schultz, J., Deichmann, R., Friston, K., & Dolan, R. J. (2004). Dissociable roles of ventral and dorsal striatum in instrumental conditioning. *Science*, *304*, 452–454. **DOI:** https://doi.org/10.1126/science.1094285, **PMID:** 15087550

O'Hare, J. K., Ade, K. K., Sukharnikova, T., Van Hooser, S. D., Palmeri, M. L., Yin, H. H., et al. (2016). Pathway-specific striatal substrates for habitual behavior. *Neuron*, *89*, 472–479. **DOI:** https://doi.org/10.1016/j.neuron.2015.12.032, **PMID:** 26804995, **PMCID:** PMC4887103

Parron, C., & Save, E. (2004). Evidence for entorhinal and parietal cortices involvement in path integration in the rat. *Experimental Brain Research*, *159*, 349–359. **DOI:** https://doi.org/10.1007/s00221-004-1960-8, **PMID:** 15526193

Paxinos, G., & Watson, C. (2014). *The rat brain in stereotaxic coordinates* (7th ed.). San Diego: Elsevier.

Pothuizen, H. H. J., Aggleton, J. P., & Vann, S. D. (2008). Do rats with retrosplenial cortex lesions lack direction? *European Journal of Neuroscience*, *28*, 2486–2498. **DOI:** https://doi.org/10.1111/j.1460-9568.2008.06550.x, **PMID:** 19032585

Powell, A. L., Nelson, A. J. D., Hindley, E., Davies, M., Aggleton, J. P., & Vann, S. D. (2017). The rat retrosplenial cortex as a link for frontal functions: A lesion analysis. *Behavioural Brain Research*, *335*, 88–102. **DOI:** https://doi.org/10.1016/j.bbr.2017.08.010, **PMID:** 28797600, **PMCID:** PMC5597037

Raichle, M. E., MacLeod, A. M., Snyder, A. Z., Powers, W. J., Gusnard, D. A., & Shulman, G. L. (2001). A default mode of brain function. *Proceedings of the National Academy of Sciences, U.S.A.*, *98*, 676–682. **DOI:** https://doi.org/10.1073/pnas.98.2.676, **PMID:** 11209064, **PMCID:** PMC14647

Reep, R. L., Cheatwood, J. L., & Corwin, J. V. (2003). The associative striatum: Organization of cortical projections to the dorsocentral striatum in rats. *Journal of Comparative Neurology*, *467*, 271–292. **DOI:** https://doi.org/10.1002/cne.10868, **PMID:** 14608594

Reep, R. L., & Corwin, J. V. (1999). Topographic organization of the striatal and thalamic connections of rat medial agranular cortex. *Brain Research*, *841*, 43–52. **DOI:** https://doi.org/10.1016/S0006-8993(99)01779-5, **PMID:** 10546986

Rothwell, P. E., Hayton, S. J., Sun, G. L., Fuccillo, M. V., Lim, B. K., & Malenka, R. C. (2015). Input- and output-specific regulation of serial order performance by corticostriatal circuits. *Neuron*, *88*, 345–356. **DOI:** https://doi.org/10.1016/j.neuron.2015.09.035, **PMID:** 26494279, **PMCID:** PMC4618801

Satyshur, M. D., Layden, E. A., Gowins, J. R., Buchanan, A., & Gollan, J. K. (2018). Functional connectivity of reflective and brooding rumination in depressed and healthy women. *Cognitive, Affective, & Behavioral Neuroscience*, *18*, 884–901. **DOI:** https://doi.org/10.3758/s13415-018-0611-7, **PMID:** 29949111

Selemon, L. D., & Goldman-Rakic, P. S. (1985). Longitudinal topography and interdigitation of corticostriatal projections in the rhesus monkey. *Journal of Neuroscience*, *5*, 776–794. **DOI:** https://doi.org/10.1523/JNEUROSCI.05-03-00776.1985, **PMID:** 2983048, **PMCID:** PMC6565017

Selemon, L. D., & Goldman-Rakic, P. S. (1988). Common cortical and subcortical targets of the dorsolateral prefrontal and posterior parietal cortices in the rhesus monkey: Evidence for a distributed neural network subserving spatially guided behavior. *Journal of Neuroscience*, *8*, 4049–4068. **DOI:** https://doi.org/10.1523/JNEUROSCI.08-11-04049.1988, **PMID:** 2846794, **PMCID:** PMC6569486

Shibata, H., Kondo, S., & Naito, J. (2004). Organization of retrosplenial cortical projections to the anterior cingulate, motor, and prefrontal cortices in the rat. *Neuroscience Research*, *49*, 1–11. **DOI:** https://doi.org/10.1016/j.neures.2004.01.005, **PMID:** 15099698

Shibata, H., & Naito, J. (2008). Organization of anterior cingulate and frontal cortical projections to the retrosplenial cortex in the rat. *Journal of Comparative Neurology*, *506*, 30–45. **DOI:** https://doi.org/10.1002/cne.21523, **PMID:** 17990270

Shulman, G. L., Fiez, J. A., Corbetta, M., Buckner, R. L., Miezin, F. M., Raichle, M. E., et al. (1997). Common blood flow changes across visual tasks: II. Decreases in cerebral cortex. *Journal of Cognitive Neuroscience*, *9*, 648–663. **DOI:** https://doi.org/10.1162/jocn.1997.9.5.648, **PMID:** 23965122

Sleezer, B. J., Castagno, M. D., & Hayden, B. Y. (2016). Rule encoding in orbitofrontal cortex and striatum guides selection. *Journal of Neuroscience*, *36*, 11223–11237. **DOI:** https://doi.org/10.1523/JNEUROSCI.1766-16.2016, **PMID:** 27807165, **PMCID:** PMC5148240

Sugar, J., Witter, M. P., van Strien, N. M., & Cappaert, N. L. M. (2011). The retrosplenial cortex: Intrinsic connectivity and connections with the (para)hippocampal region in the rat. An interactive connectome. *Frontiers in Neuroinformatics*, *5*, 7. **DOI:** https://doi.org/10.3389/fninf.2011.00007, **PMID:** 21847380, **PMCID:** PMC3147162

Sutherland, R. J., Wishaw, I. Q., & Kolb, B. (1988). Contributions of cingulate cortex to two forms of spatial learning and memory. *Journal of Neuroscience*, *8*, 1863–1872. **DOI:** https://doi.org/10.1523/JNEUROSCI.08-06-01863.1988, **PMID:** 3385478, **PMCID:** PMC6569344

Tabuchi, E., Furusawa, A. A., Hori, E., Umeno, K., Ono, T., & Nishijo, H. (2005). Neural correlates to action and rewards in the rat posterior cingulate cortex. *NeuroReport*, *16*, 949–953. **DOI:** https://doi.org/10.1097/00001756-200506210-00014, **PMID:** 15931067

Upadhyay, J., Baker, S. J., Chandran, P., Miller, L., Lee, Y., Marek, G. J., et al. (2011). Default-mode-like network activation in awake rodents. *PLoS One*, *6*, e27839. **DOI:** https://doi.org/10.1371/journal.pone.0027839, **PMID:** 22125628, **PMCID:** PMC3220684

Valenstein, E., Bowers, D., Verfaellie, M., Heilman, K. M., Day, A., & Watson, R. T. (1987). Retrosplenial amnesia. *Brain*, *110*, 1631–1646. **DOI:** https://doi.org/10.1093/brain/110.6.1631, **PMID:** 3427404

van Groen, T., & Wyss, J. M. (1990). Connections of the retrosplenial granular a cortex in the rat. *Journal of Comparative Neurology*, *300*, 593–606. **DOI:** https://doi.org/10.1002/cne.903000412, **PMID:** 2273095

van Groen, T., & Wyss, J. M. (1992). Connections of the retrosplenial dysgranular cortex in the rat. *Journal of Comparative Neurology*, *315*, 200–216. **DOI:** https://doi.org/10.1002/cne.903150207, **PMID:** 1545009

van Groen, T., & Wyss, J. M. (2003). Connections of the retrosplenial granular b cortex in the rat. *Journal of Comparative Neurology*, *463*, 249–263. **DOI:** https://doi.org/10.1002/cne.10757, **PMID:** 12820159

Vann, S. D., & Aggleton, J. P. (2002). Extensive cytotoxic lesions of the rat retrosplenial cortex reveal consistent deficits on tasks that tax allocentric spatial memory. *Behavioral Neuroscience*, *116*, 85–94. **DOI:** https://doi.org/10.1037/0735-7044.116.1.85, **PMID:** 11895186

Vann, S. D., & Aggleton, J. P. (2004). Testing the importance of the retrosplenial guidance system: Effects of different sized retrosplenial cortex lesions on heading direction and spatial working memory. *Behavioural Brain Research*, *155*, 97–108. **DOI:** https://doi.org/10.1016/j.bbr.2004.04.005, **PMID:** 15325783

Vann, S. D., Aggleton, J. P., & Maguire, E. A. (2009). What does the retrosplenial cortex do? *Nature Reviews Neuroscience*, *10*, 792–802. **DOI:** https://doi.org/10.1038/nrn2733, **PMID:** 19812579

Vedder, L. C., Miller, A. M. P., Harrison, M. B., & Smith, D. M. (2017). Retrosplenial cortical neurons encode navigational cues, trajectories and reward locations during goal directed navigation. *Cerebral Cortex*, *27*, 3713–3723. **DOI:** https://doi.org/10.1093/cercor/bhw192, **PMID:** 27473323, **PMCID:** PMC6059095

Verwer, R. W. H., Meijer, R. J., Van Uum, H. F. M., & Witter, M. P. (1997). Collateral projections from the rat hippocampal formation to the lateral and medial prefrontal cortex. *Hippocampus*, *7*, 397–402. **DOI:** https://doi.org/10.1002/(SICI)1098-1063(1997)7:4<397::AID-HIPO5>3.0.CO;2-G, **PMID:** 9287079

Voorn, P., Vanderschuren, L. J. M. J., Groenewegen, H. J., Robbins, T. W., & Pennartz, C. M. A. (2004). Putting a spin on the dorsal–ventral divide of the striatum. *Trends in Neurosciences*, *27*, 468–474. **DOI:** https://doi.org/10.1016/j.tins.2004.06.006, **PMID:** 15271494

Wisner, K., Odintsov, B., Brozoski, D., & Brozoski, T. J. (2016). Ratat1: A digital rat brain stereotaxic atlas derived from high-resolution MRI images scanned in three dimensions. *Frontiers in Systems Neuroscience*, *10*, 64. **DOI:** https://doi.org/10.3389/fnsys.2016.00064, **PMID:** 27540358, **PMCID:** PMC4973504

Wu, H., Sun, H., Xu, J., Wu, Y., Wang, C., Xiao, J., et al. (2016). Changed hub and corresponding functional connectivity of subgenual anterior cingulate cortex in major depressive disorder. *Frontiers in Neuroanatomy*, *10*, 120. **DOI:** https://doi.org/10.3389/fnana.2016.00120, **PMID:** 28018183, **PMCID:** PMC5159433

Yeo, B. T. T., Krienen, F. M., Sepulcre, J., Sabuncu, M. R., Lashkari, D., Hollinshead, M., et al. (2011). The organization of the human cerebral cortex estimated by intrinsic functional connectivity. *Journal of Neurophysiology*, *106*, 1125–1165. **DOI:** https://doi.org/10.1152/jn.00338.2011, **PMID:** 21653723, **PMCID:** PMC3174820

Yin, H. H., & Knowlton, B. J. (2004). Contributions of striatal subregions to place and response learning. *Learning & Memory*, *11*, 459–463. **DOI:** https://doi.org/10.1101/lm.81004, **PMID:** 15286184, **PMCID:** PMC498333

Yin, H. H., Knowlton, B. J., & Balleine, B. W. (2006). Inactivation of dorsolateral striatum enhances sensitivity to changes in the action-outcome contingency in instrumental conditioning. *Behavioural Brain Research*, *166*, 189–196. **DOI:** https://doi.org/10.1016/j.bbr.2005.07.012, **PMID:** 16153716

Yin, H. H., Ostlund, S. B., Knowlton, B. J., & Balleine, B. W. (2005). The role of the dorsomedial striatum in instrumental conditioning. *European Journal of Neuroscience*, *22*, 513–523. **DOI:** https://doi.org/10.1111/j.1460-9568.2005.04218.x, **PMID:** 16045504